Metastatic Phenotype in CWR22 Prostate Cancer Xenograft Following Castration

Steven J. Seedhouse,[1] Hayley C. Affronti,[2] Ellen Karasik,[1] Bryan M. Gillard,[1] Gissou Azabdaftari,[3] Dominic J. Smiraglia,[2] and Barbara A. Foster[1]*

[1]*Department of Pharmacology and Therapeutics, Roswell Park Cancer Institute, Buffalo, New York*
[2]*Department of Cancer Genetics, Roswell Park Cancer Institute, Buffalo, New York*
[3]*Department of Pathology, Roswell Park Cancer Institute, Buffalo, New York*

BACKGROUND. CWR22 is a human xenograft model of primary prostate cancer (PCa) that is often utilized to study castration recurrent (CR) PCa. CWR22 recapitulates clinical response to androgen deprivation therapy (ADT), in that tumors regress in response to castration, but can recur after a period of time.

METHODS. Two cohorts of mice, totaling 117 mice were implanted with CWR22, allowed to develop tumors, castrated by pellet removal and followed for a period of 32 and 50 weeks. Mice presenting with tumors $>2.0\,cm^3$ at the primary site, moribund appearance, or palpable masses other than the primary tumor were sacrificed prior to the endpoint of the study. Tumor tissue, serum, and abnormal lesions were collected upon necropsy and analyzed by IHC, H&E, and PCR for presence of metastatic lesions arising from CWR22.

RESULTS. Herein, we report that CWR22 progresses after castration from a primary, hormonal therapy-naïve tumor to metastatic disease in 20% of castrated nude mice. Histological examination of CWR22 primary tumors revealed distinct pathologies that correlated with metastatic outcome after castration.

CONCLUSION. This is the first report and characterization of spontaneous metastasis in the CWR22 model, thus, CWR22 is a bona-fide model of clinical PCa representing the full progression from androgen-sensitive, primary PCa to metastatic CR-PCa. *Prostate 76:359–368, 2016.* © 2015 The Authors. *The Prostate* published by Wiley Periodicals, Inc.

KEY WORDS: **CWR22; CWR22R; prostate cancer; metastasis; xenograft**

INTRODUCTION

The NCI estimates that more than 230 000 men were diagnosed with prostate cancer (PCa) in 2014, with mortality reaching nearly 30,000 [1]. Primary PCa is treated with radical prostatectomy but 22% of patients experience biochemical recurrence and disseminated disease within 5 years of surgery [2]. Upon recurrence, second-line androgen deprivation therapy (ADT) reduces circulating PSA levels in 80–90% of patients while also reducing bone pain and metastatic tumor burden [3]. When patients' tumors no longer respond to ADT, their cancers are referred to as castration recurrent (CR) disease. At this late-stage of CR-PCa, treatments historically comprised palliative chemotherapies like docetaxel [4,5], however, there have been many promising recent developments for

Grant sponsor: BAF National Institute of Health; Grant number: 5R01CA095367; Grant sponsor: Roswell Park Alliance Foundation; Grant sponsor: National Cancer Institute; Grant number: 2P30CA016056; Grant sponsor: DJS American Institute of Cancer Research; Grant number: 208739.

[The copyright line of this article was changed in January 2016 after original online publication.]

Steven J. Seedhouse and Hayley C. Affronti contributed equally to this work.

Conflicts of Interest: The authors declare no conflicts of interest.

*Correspondence to: Barbara A. Foster, Roswell Park Cancer Institute, Elm & Carlton Streets, CGP L4-322, Buffalo, NY 14263.
E-mail: barbara.Foster@RoswellPark.org

Received 19 August 2015; Accepted 13 November 2015
DOI 10.1002/pros.23127
Published online 8 December 2015 in Wiley Online Library (wileyonlinelibrary.com).

CR-PCa treatment, such as abiraterone acetate and enzalutamide [6–12]. Improved understanding of the transition from primary to metastatic PCa at a mechanistic and molecular level will spur continued development of novel therapies for CR, metastatic PCa. Models that recapitulate the transition from primary to metastatic disease are therefore needed to enable such studies.

Various model systems are available to facilitate studies of CR-PCa and metastasis, including both cell culture and animal models. For example, LNCaP-C4-2 is a castration-recurrent cell line obtained from tumors grown in castrated mice derived from an androgen-sensitive parental cell line LNCaP, which originates from a lymph node metastasis [13–15]. This isogenic pair provides a system to compare androgen-sensitive prostate cancer to castration recurrence. Other cell lines provide systems for studying metastatic disease. For instance, PC-3 is a cell line originally derived from a bone lesion and metastasizes when grafted in immunocompromised mice [16,17]. While this property enables studies of the metastatic phenotype, PC-3 cells do not undergo a transition from primary to metastatic disease as PC-3, like LNCaP, is originally derived from a metastatic lesion.

In addition to cell lines, several genetically engineered mouse models (GEMMs) progress to metastatic disease and represent poorly differentiated, aggressive PCa such as LADY [18] and TRAMP [19]. More recently, several GEMMs have been developed that recapitulate molecular changes observed in clinical prostate cancer such as the Hi-Myc [20] and prostate-specific $Pten^{-/-}$ models [21] in that they exhibit early PIN lesions that progress to adenocarcinoma, and in the case of $Pten^{-/-}$ can result in metastatic disease.

While GEMMs provide certain advantages such as growth in endogenous environment while transitioning from normal to malignant phenotypes in the presence of an immune system, human xenograft models can provide other advantages such as providing a replenishable source of human tissue for study of tumor response to therapies. One popular xenograft model that accurately recapitulates certain features of clinical PCa is the CWR22 xenograft model. Originally reported in 1993, CWR22 was derived from a hormonal therapy naïve, primary PCa specimen in a patient that also had bone metastasis [22]. The original CWR22 tumor sample was transplanted as fresh minced tumor initially and has since been passaged as either fresh or frozen cell suspensions in either PBS or matrigel, but has not been maintained as a cell line in culture. While CWR22 can grow in various tissue implantation sites, it is most commonly used as a subcutaneous xenograft [23]. CWR22 xenografts make and secrete PSA into the circulation of host mice, with circulating PSA levels falling rapidly and dramatically if tumors are resected or if mice are castrated. Tumors also regress substantially in size in response to castration [24]. After a period of several months, CWR22 tumors can recur in a castrate setting accompanied by a rise in circulating PSA. Response to castration is variable with some mice apparently cured (without primary tumor recurrence), while others have relapse with primary tumor regrowth between 3 and 10 months post castration [24].

Potential mechanisms for recurrence in castrated CWR22 have been reported such as an increase in AR expression levels, as well as novel AR mutations [7,25]. One mutation results in a ligand binding domain-null AR that is constitutively nuclear [25]. A clonal cell line derived from one such recurrent tumor, termed CWR22R*v1*, carries this mutation. While the CWR22 model has never before been reported to progress to metastatic disease, the CWR22R*v1* cell line can metastasize if grafted into immunocompromised mice indicating the CWR22 model has the capacity to yield clones with metastatic propensity [26].

Here we report CWR22 progression from primary, hormone therapy-naïve PCa to CR disease with kinetics similar to previous reports, but with the novel discovery of metastases to multiple sites. Metastasis was observed in 20% of castrated mice and metastatic outcome correlates with a distinct histological phenotype. These findings represent the utility of the CWR22 model to study the full spectrum of disease from androgen sensitive to CR-PCa to metastatic disease. Ultimately, these results will provide researchers with a better knowledge for designing studies using the CWR22 model and are an important addition to the arsenal of models available to researchers studying disease progression in PCa.

MATERIALS AND METHODS

Study Design

Nude mice were surgically castrated and silastic tubing containing 12.5 mg testosterone for sustained release was implanted. After 2 weeks allowing circulating testosterone levels to equilibrate, 1×10^6 CWR22 cells in matrigel were injected into the right flank of nude mice. CWR22 cells were obtained from fresh resected CWR22 tumors and dissociated to make matrigel suspensions. Beginning 1 week after grafting, tumor measurements were taken with calipers and tumor sizes were calculated using the formula (length^2 $\times$ width $\times$ 0.5234). When tumors reached $\sim$250 mm^3 in size, mice were experimentally castrated by removing the testosterone tubing.

Tumors were measured weekly and serum collected monthly for up to 32-weeks (cohort 1) or 50 weeks (cohort 2) post-castration unless mice needed to be euthanized prior to termination of the study. At euthanasia, primary tumor, and any metastatic or suspected metastatic tissue were collected.

CWR22 Xenograft

5×10^6 CWR22 cells from frozen cell stocks were pelleted, resuspended in 100 μl matrigel, and injected into the right flank of nude mice. After tumors reached ~1000 mm^3, mice were euthanized and tumors were excised and disassociated with proteases in RPMI 1640 + 20% fetal calf serum. Tumor digests were resuspended at a concentration of 1×10^7 cells/ml in matrigel, and 1×10^6 cells were injected in a volume of 100 μl subcutaneously into right flank of nude mice to initiate study. All mice were housed and cared for under the defined guidelines of the Institutional Animal Care and Use Committee (IACUC) in the Department of Laboratory and Animal Resource (DLAR) core facility at Roswell Park Cancer Institute (RPCI).

Tissue Collection

Mice were monitored several times weekly and euthanized when tumor sizes reached >1000 mm^3, or when a metastatic tumor could be palpated in the abdomen, or when the mouse was moribund (typically presenting with ascites). At euthanasia, primary tumors were resected and processed by formalizing fixation and paraffin embedding (FFPE) or snap frozen in liquid nitrogen for future analysis of RNA/DNA/Protein. Frozen tissues and serum samples were stored at −80°C until use. Where mice presented with evidence of gross metastasis, selected organs were harvested and processed for histology or snap frozen.

Immunohistochemistry

Freshly harvested tissues were fixed by submerging in 10% buffered formalin (Fisher Scientific, Kalamazoo, MI) for 24 hr prior to processing. Tissues were then embedded in paraffin using a Leica Modular Tissue Embedding Center (Leica, Buffalo Grove, IL) and sliced in 5 μm sections using a Manual Rotary Microtome (Leica, Buffalo Grove, IL). Slides were de-parafinized by several incubations in xylenes and then rehydrated in graded alcohols followed by H_2O. Slides were incubated in 1x citrate buffer, pH 6 (Invitrogen/Thermo Fisher, Grand Island, NY) for 20 min then in 3% H_2O_2 for 15 min. To block non-specific binding, tissues were incubated with 10% normal goat serum for 30 min, followed by avidin/biotin block (Vector Labs, Burlingame, CA). Primary antibodies were incubated at the following dilutions: Ki67 (1:500, Leica, Buffalo Grove, IL), Synaptophysin (1:400, Zymed, South San Francisco, CA), and AR (1:200, Millipore, Billerica, MA) in 1% BSA solution and incubated for 30 min at room temperature, followed by incubation with biotinylated goat anti rabbit secondary antibody for 15 minutes. For signal enhancement, ABC reagent (Vector Labs, Burlingame, CA) was applied for 30 min. Slides were incubated with 3,3′-diaminobenzidine (DAB) substrate (Dako, Carpinteria, CA) for 5 min and then counterstained with Hematoxylin (Dako, Carpinteria, CA) for 20 sec. Slides were dehydrated through several baths of graded alcohols and xylenes and then coverslipped.

Hoechst 33258 Staining

Freshly harvested tissues were fixed by submerging in 10% buffered formalin for 24 hr prior to processing. Tissues were then embedded in paraffin and sliced in 5 μm serial sections and mounted on glass slides. Slides were deparaffinised in xylenes, rehydrated through a graded series of alcohol washes, and equilibrated in PBS. 20 μg/ml Hoechst 33,258 solution in PBS was used to stain tissue on the slides. Slides were then coverslipped using Vectashield without DAPI (Vector Lab, Burlingame, CA).

Isolation of RNA From Frozen Tissue

Flash Frozen tissue chunks were removed from −80°C and approximately 20 mg tissue was homogenized using a Polytron PT 2100 tissue homogenizer (Cardinal Health, Dublin, OH) in 1mL TRIzol (Thermo Fisher, Grand Island, NY). RNA was isolated from homogenized solutions using Ribopure RNA Purification Kit (Thermo Fisher, Grand Island, NY) as per manufacturer's protocol. Isolated RNA was then treated with DNAse using TURBO DNAfree it (Thermo Fisher, Grand Island, NY), as per the manufacturer's protocol. Isolated RNA was quantified and checked for integrity and purity (260:280 ratio) using NANOdrop 8,000 Spectrophotometer (Thermo Scientific, Wilmington, DE).

RT, qPCR and PCR

Five hundred nanogram RNA was used to generate cDNA libraries using random hexamer primers, and SuperScript III First Strand cDNA synthesis kits (Thermo Fisher, Grand Island, NY) as per manufacturer's protocol. cDNA libraries were diluted 1:5 in DEPC-treated H_2O for use in qPCR experiments. All

qPCR experiments from cell lines and mouse tissue were conducted in 20 μl reaction volumes in 96-well format on an ABI 7300 Real-Time PCR system (Thermo Fisher, Grand Island, NY). Each sample was measured in triplicate using Half Skirt 96-well PCR Plated (VWR, Radnor, PA) sealed with MicroAmp Optical Adhesive Film (Thermo Fisher, Grand Island, NY), and Taqman Universal PCR mastermix, no AMPerase UNG (Thermo Fisher, Grand Island, NY). Gene expression was normalized using ΔΔCT method to an appropriate endogenous control as indicated. Taqman primers/probes (Thermo Fisher, Grand Island, NY) used were as follows: 18s rRNA, Hs 03003631_g1; CDH1, Hs01023894_m1; VIM, Hs001855 84_m1; KRT8, Hs01595539_g1; P63, Hs00978343_m1; CD24, Hs03044178_g1; CD44, Hs01075861_m1. Human β-actin primers: fwd—5′-ACAGAGCCTCGCCT TTGC, rev—5′-GGAATCCTTCTGACCCATG. Mouse β-actin primers: fwd—5′-CAGCTTCTTTGCAGCTCC TTC, rev—5′-ACCCATTCCCACCATCACAC.

Testosterone Levels

A cohort of six mice was evaluated by collecting blood by either orbital eye bleed or cardiac puncture (at euthanasia) at three time points: at testosterone implant, at tumor graft, and 4 weeks post castration when mice were euthanized. Blood was centrifuged in Z-gel microtubes (Sarstedt, Germany) to obtain serum and frozen at −80°C. Frozen serum samples were sent to the Research Testing Services Endocrinology Laboratory at Cornell University College of Veterinary Medicine for determination of testosterone levels.

RESULTS

CWR22 Xenograft Outcome

In order to study in detail the variable response to castration in the CWR22 model, we designed an experiment to follow a large cohort of mice over a period of months following castration. Nude mice (13 w.o.) were surgically castrated and silastic tubing containing testosterone was implanted. After 2 weeks testosterone levels equilibrated at 10–15 ng/ml (Supplementary material SI-1), at which time CWR22 cells were injected. When tumors reached ~250 mm^3 in size, mice were experimentally castrated by removing the testosterone implant, which reduced serum testosterone levels below the limit of detection (0.04 ng/ml) by 4 weeks post castration. For cohort 1 (n = 51), tumors were measured weekly post castration for up to 32-weeks unless mice needed to be euthanized earlier due to development of a large tumor or they became moribund. For cohort 2 (n = 66), mice were allowed to age up to 50 weeks post castration (Fig. 1). At euthanasia, primary tumors were weighed and as expected, tumor weight strongly correlated with final tumor caliper measurement, verifying the accuracy of our tumor measurements as a method used throughout the study for estimating bulk tumor size, and therefore recurrence (Supplementary material SI-2).

We defined "primary recurrence" as tumor reaching greater than 500 mm^3 post-castration at the injection site (primary tumor), a "stable disease" as tumor between 100 and 500 mm^3, and "no recurrence" of primary tumor as tumor measuring less than 100 mm^3. Primary tumors began to recur by 4 weeks post-castration in both cohorts (Fig. 2A). Recurrences continued to present up to study completion in cohort 1 (32 weeks post-castration), and up to 44 weeks (~10 months) post-castration in cohort 2 (Fig. 2A), consistent with the earliest findings in this model [24].

Evidence of Gross Metastases

The CWR22 xenograft model has never before been reported to lead to metastatic disease. However, we report here that some mice died with metastasis post

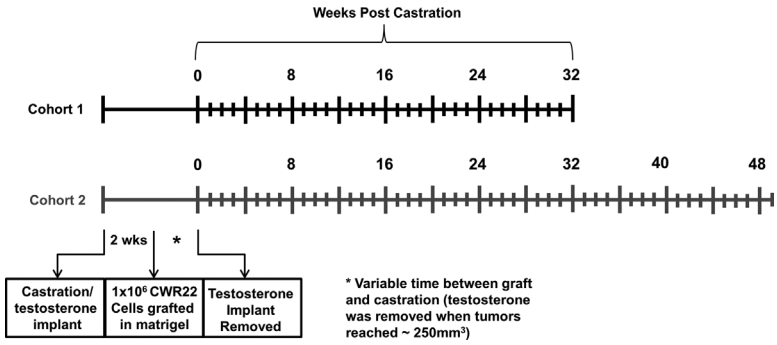

Fig. 1. Experimental design for two CWR22 cohorts in this study. At study inception, mice (13 w.o.) were castrated and silastic tubing with testosterone for sustained released are implanted in the back between the shoulders. After 2 weeks, 1 million CWR22 tumor cells in matrigel were injected into the right flank of mice. Once tumors reached ~250 mm^3, testosterone tubing was removed and mice were followed for 32 weeks (cohort 1) or 50 weeks (cohort 2).

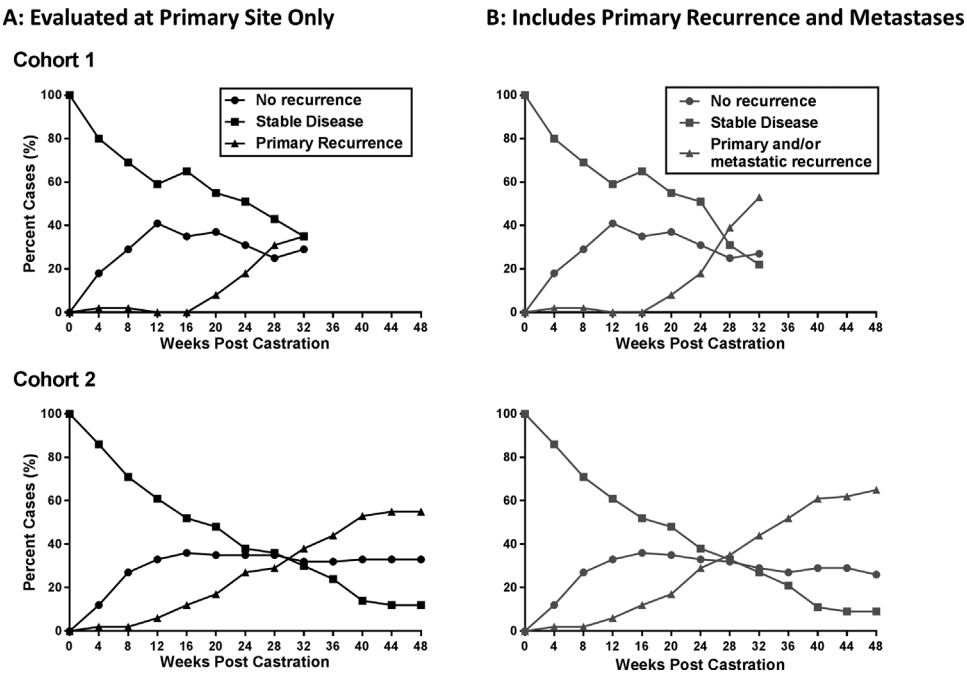

Fig. 2. Primary tumor recurrence was determined at 4 week intervals defining recurrence only by primary tumor outcome (**A**), or with consideration of metastatic outcome (**B**).

castration. For both cohorts, some mice exhibited symptoms of metastatic disease including severe ascites and otherwise moribund appearance. Mice were euthanized when presenting with these symptoms or in several cases, when tumors distinct from the primary subcutaneous site could be palpated in their abdomen. Upon necropsy, various organs were inspected and resected if they appeared to harbor overt metastatic lesions. H&E staining of sections of the suspected metastases revealed abnormal pathology in multiple organ sites (Fig. 3).

While histopathological characterization suggested presence of tumor, in order to determine if these lesions were in fact metastases derived from the primary human tumor cells, mouse- and human-specific β-actin RT-PCR primers were designed and species specificity was validated (Supplementary material SI-3). Expression analysis for human β-actin confirmed human cells at most sites of suspected metastases, indicating that they arose from the primary xenograft (Fig. 4). Additionally, several suspected metastatic lesions tested negative for human β-actin by RT-PCR, indicating they did not contain cells of human origin. To confirm these results, Hoechst 33258 dye staining was performed on tissue sections from these suspected metastases (Supplementary material SI-4). Hoechst 33,258 can distinguish human from mouse nuclei by visualization of punctate fluorescence upon DNA binding of Hoechst dye in mouse nuclei, and diffuse, faded fluorescence in human nuclei [27]. Some tumors were of clear human origin with intermixed mouse stroma while, others were comprised entirely of mouse cells. These results further confirmed and validated our RT-PCR analysis of human and mouse β-actin. Pathological review of H&E sections of tumors comprised entirely of mouse cells indicated that some were mouse lymphomas (Supplementary material SI-5). Lymphoma in nude mice carrying human xenografts has been reported at a rate of 7% in mice >5 months old [28]. We determined the incidence of lymphoma in the longest study (cohort 2) was 10%. Consequently, all mice presenting with tumors not of human origin were censored from our analyses (Table I).

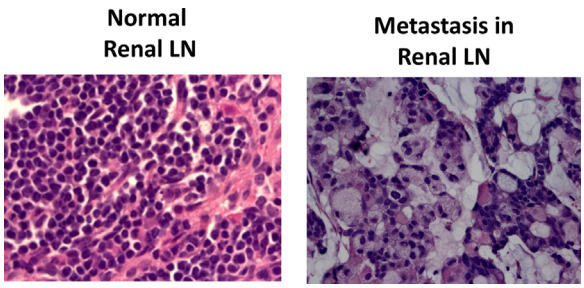

Fig. 3. Histopathology of normal renal lymph node and metastatic renal lymph node in a CWR22 grafted mouse.

CWR22 Primary and Metastatic Recurrence Rates

For mice that presented with metastases, we term this outcome "metastatic recurrence", which therefore

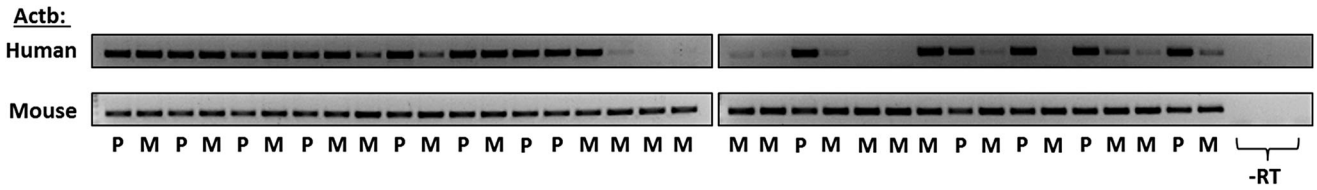

Fig. 4. RT-PCR screening of suspected metastatic lesions in cohort I using human β-actin primers revealed detectable human cells in suspected metastases. Each lane represents a separate metastatic lesion.

makes the overall recurrence rates (at the primary site and/or the metastatic site) higher than what is reflected by measurement of primary tumor alone (Fig. 2A vs. B triangles). By week 32 in cohort 1, the recurrence rate at the primary site was 35%, while the metastatic recurrence rate was 29%, for a combined recurrence rate of 53%. Similarly, by week 32 in cohort 2 the recurrence rates at the primary site was 38%, while the metastatic recurrence rate was 12%, for a combined recurrence rate of 44%. Some mice that had a primary site recurrence also develop metastases and therefore the recurrence rates at the primary site added to the metastatic recurrence rate are not equal to the combined recurrence rate discussed above. Notably, there was no change in stable disease rates.

The impact of metastasis on primary tumor growth kinetics was examined. Overall, mice with metastases had a lower recurrence rate at the primary site than mice without metastasis. Combining the two cohorts, we find that the recurrence rate at the primary site was 34.7% in mice with metastases compared to 65.9% in mice void of metastatic lesions. Furthermore, termination of the study at 32 weeks (cohort 1) evidently misses some recurrences that would eventually happen between 32 and 44 weeks post-castration (cohort 2). The recurrence rate for this model could therefore be substantially underestimated without extended observation and monitoring for metastasis.

TABLE I. Total Experimental Numbers for Mice in Each Cohort

Outcome:	Cohort 1	Cohort 2
Total non-censored	51	66
Censored	20	14
Recurrent tumor (>500 mm^3)	27	43
Stable disease	11	6
No recurrence	13	17
Lymphoma	N/A	7
Metastases	15	8

Animals were censored due to death unrelated to disease, lymphoma or lack of initial primary tumor development prior to castration. It is important to note that animals that developed metastases are also incorporated in the categories describing primary tumor recurrence.

For example, recurrence rate without consideration for metastasis is 35-38% at week 32 (in cohorts 1 and 2 respectively). However, overall recurrence rate including metastasis is 65% by 48 weeks (at study completion, cohort 2).

Location of Metastases

The overall incidence of confirmed metastases was 20% (23/117). Lesions were predominantly found in lymph nodes (n = 13) including the renal hilum, mesentery, pelvic, and one in the submandibular lymph nodes but also included other distant organ sites (Table II), most often the pancreas (n = 9) spleen (n = 3) and lung (n = 3). Some mice presented with multiple metastases. Additional micrometastases in other organs cannot be ruled out, as only organs displaying gross signs of metastasis were harvested and evaluated by IHC and RT-PCR. Because human PCa often metastasizes to bone, all of the mice in cohort 2 (n = 66) were examined by Faxitron and suspicious lesions were examined by H&E staining of ribs and spine and found no evidence of bone metastasis (data not shown).

Molecular Analysis of Metastases

Primary tumors from mice (C1) with and without metastatic lesions were characterized for expression

TABLE II. Location of RT-PCR Confirmed Metastases (Some Mice Presented With Multiple Lesions)

Location of metastatic lesion	# Observed
Lymph node (renal hilum, mesentery, submandibular, pelvic)	13
Pancreas	9
Spleen	3
Lung	3
Stomach	1
Liver	1
Kidney	1
Mesentary	1

of various markers by qRT-PCR, including E-cadherin, Vimentin, p63, Cytokeratin 8, CD24, and CD44. Tumors from mice with and without metastases did not differentially express any of the markers evaluated by qRT-PCR (Supplementary material SI-6A–C). Histological evaluation of primary tumors was then performed and two distinct phenotypes were identified. Mice that presented with metastases more often had primary tumors composed of mucin-producing, signet ring cells (phenotype 2) or mixed phenotypes (1 and 2), as compared to non-metastatic mice ($P < 0.001$, χ^2 test), which tended to have more uniform, well differentiated tumors (phenotype 1) (Fig. 5). Highly focal positive synaptophysin (SYP) staining and heterogeneous or negative AR staining characterized phenotype 2 ($P < 0.001$, χ^2 test), while high, uniform AR staining and low SYP staining characterized phenotype 1 ($P < 0.001$, χ^2 test, Fig. 6). Together, these data indicate that primary tumors with phenotype 2 or mixed phenotypes, and SYP-high, AR-low expression have a significantly higher propensity to metastasize in the CWR22 model.

DISCUSSION

Various transgenic mouse models exist that accurately reflect early stage, prostate cancer (e.g., Pten$^{-/-}$, Hi-Myc) and late-stage, aggressive PCa (e.g., TRAMP) [19–21]. In addition, some human PCa cell lines derived from metastatic tissue (e.g., PC-3) metastasize when grafted in nude mice [16,17]. While human cell lines are very valuable for studying a particular phenotype and stage, they fall short in modeling the transition to advanced disease typified by castration recurrence and metastasis. Furthermore, the existing transgenic mouse models effectively mimic clinical PCa, but would be well complemented by accurate human xenograft models to study disease progression mechanistically in human tumor cells. Herein we report that the CWR22 xenograft model, which is initially derived from a primary androgen sensitive tumor, can progress to metastatic disease in the castrate environment. Moreover, among a cohort of implanted mice, there are variable outcomes with respect to primary tumor responses, and metastatic outcome. Primary tumors in mice that presented with metastases were SYP-high, AR-low, and composed of mucin-

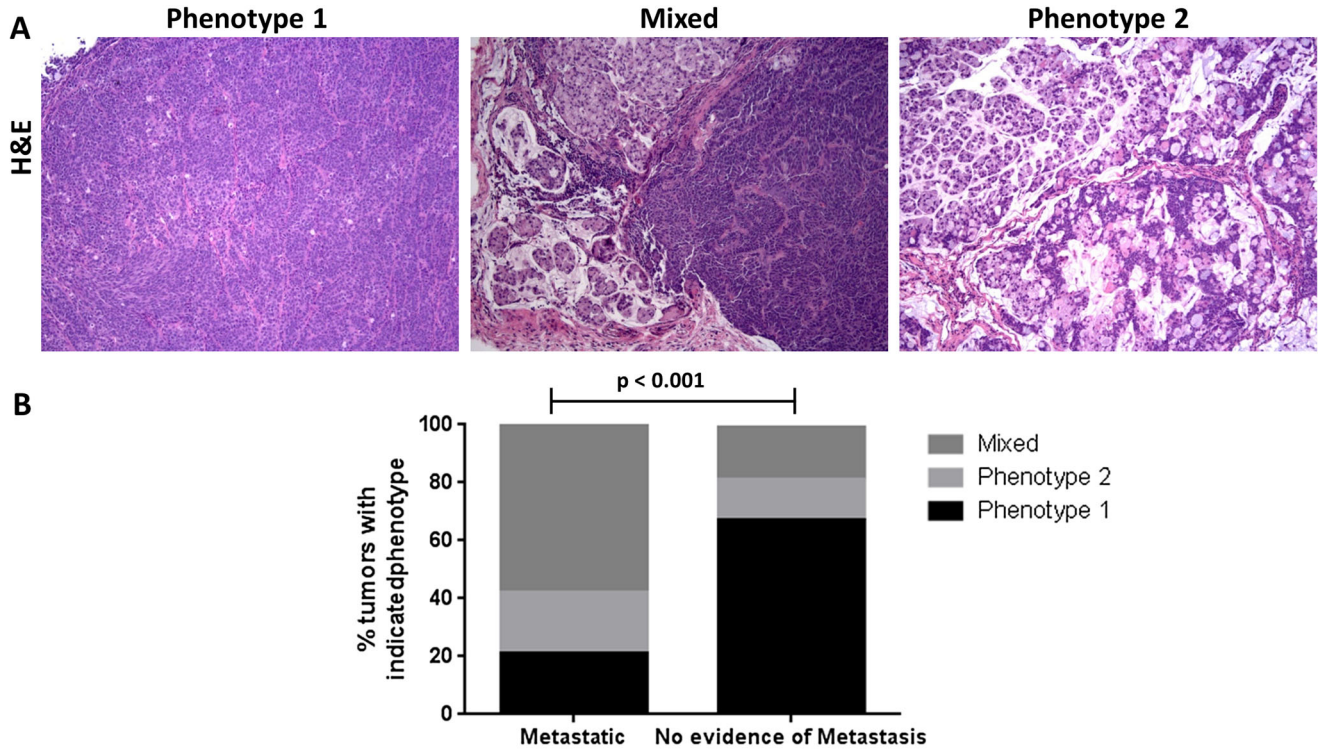

Fig. 5. H&E slides of all primary tumors were scored according to two clear and distinct phenotypes (1 and 2). (**A**) Tumors were classified as phenotype 1, phenotype 2, or mixed if there was a >10% prevalence of both phenotypes in histological sections. (**B**) Mice with metastases had a higher proportion of primary tumors with phenotype 2 including a mixed phenotype, as compared to mice without metastases, which predominantly comprised phenotype 1 primary tumors ($P < 0.001$ by χ^2 test). Mice without primary tumors (i.e., apparent cures) are necessarily excluded from analysis.

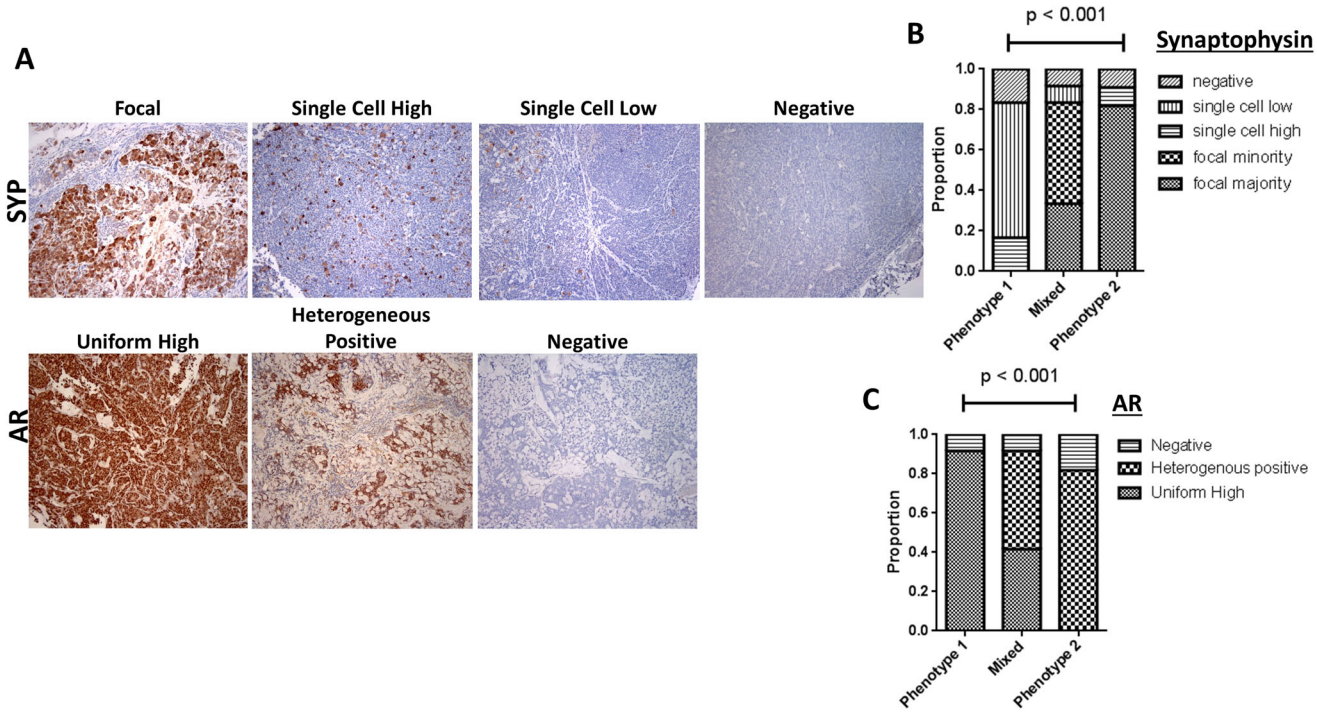

Fig. 6. Molecular differences between phenotypes were explored by IHC analysis of AR and SYP expression. (**A**) Scoring system used for evaluation of IHC slides for AR and SYP expression in all primary tumors. (**B**) SYP positivity increased in mixed and phenotype 2 tumors relative to phenotype 1, which primarily had single cell staining patterns ($P < 0.001$, χ^2 test). (**C**) AR positivity was proportionally increased in phenotype 1 tumors relative to phenotype 2 which was more heterogeneous for AR positivity ($P < 0.001$, χ^2 test).

producing, signet ring cells. In contrast, primary tumors in mice devoid of metastases were AR-high, SYP-low, and were more histologically uniform. This extensive characterization of the CWR22 model should greatly improve our ability to study the transition and progression towards metastatic disease from a molecular and mechanistic standpoint, and also to test interventions and therapeutic approaches.

Mice that developed metastatic disease post-castration were less likely to have recurrence at the primary site. This may indicate mutually suppressive relationship between primary tumor and metastasis in this model [29]. Previous reports of this phenomenon reveal that presence of a primary tumor can suppress metastatic growth, and removal of primary tumor can allow metastatic growth [29]. Regardless of the potential mechanism by which the presence of metastasis might suppress recurrence at the primary site, these observations clearly indicate that it is insufficient to rely solely on primary tumor measurements as a determinant of recurrence following castration with the CWR22 model. Characterization of the primary tumors to identify differences among those that did, or did not spawn metastasis, identified several differences. Primary tumors that displayed predominantly "phenotype 2," a mucinous, signet ring tumor, were more likely to associate with metastasis. Furthermore, "phenotype 2" tumors were more likely to be AR low or negative, and SYP high, while "phenotype 1" tumors were AR-high and SYP-low. These data indicate that tumors with mixed histology or high prevalence of de-differentiated or transdifferentiated cell types, as evidenced by the IHC staining patterns of AR and SYP, manifest in metastasis in the CWR22 model.

Notably, the mixed histological phenotype associated with metastases mirrors what is often seen in the clinic. Poorly differentiated, heterogeneous tumors similar to those represented by phenotype 2, are known to correlate with a high gleason grade, which is associated with invasive, aggressive prostate cancer [30]. Conversely, homogeneous, well differentiated tumors similar to phenotype 1 are known to correlate with a low gleason grade, which tends to be associated with a non-invasive and less aggressive prostate cancer [30]. These features highlight the similarity between the CWR22 model and patient histological phenotype. In addition, not all patients that develop androgen sensitive prostate cancer are sensitive to castration. Nor do all patients who develop CR-PCa, develop metastases. Therefore, PCa patients can develop a variety of outcomes and it would be invaluable to have in vivo models which mirror this heterogeneity. As seen here, on average among the two studies, 60% of animals developed recurrent

disease after castration, 14% ended with stable disease carrying non-progressing small tumors at the primary site, and 26% exhibited apparent cure with no recurrence. In total, 20% of mice in the two cohorts developed metastatic disease post-castration, mostly without recurrence at the primary site. Thus, the CWR22 model is an excellent in vivo model for evaluating new therapies across a heterogeneous population with a variety of outcomes similar to that seen in the clinic.

Our study involved an initial cohort in which we first observed metastatic recurrence after castration, and a confirmatory follow-up study spanning an extended period of time post-castration to validate and expand our initial findings. Because we followed a total of 117 mice for either 32 or 50 weeks post-castration we were able to robustly measure the metastatic phenotype despite its manifestation in only 20% of mice. It is likely that this particular aspect of the CWR22 model in nude mice was not previously reported because it is rare for studies to include such large cohorts followed for such an extended period of time. It should also be noted, however, that CWR22 has been passaged multiple times since it was established and initially reported in 1993. It is possible that over time, the model has selected for a more aggressive population with a novel or at least higher metastatic propensity than the original xenograft. Importantly, our studies did in fact recapitulate classic, reported features of this model with respect to tumor response rates to castration, and time to recurrence, indicating that these aspects of the model have not changed.

One provocative question raised by our observations is whether or not castration itself induces or supports metastatic spread, or alternatively if the CWR22 model would exhibit a similar stochastic metastatic response even without castration. One difficulty in answering such a question is CWR22, like other PCa models, grows rapidly in androgen replete conditions, therefore primary tumors become too large and require animal euthanasia within a period of weeks. The notable incidence of bona fide metastasis in the CWR22 model enables such future studies and should facilitate our understanding of PCa, specifically with respect to progression from primary PCa to CR, metastatic disease.

CONCLUSIONS

Here we report, for the first time, that the CWR22 model has the ability to progress from primary androgen sensitive CaP to metastatic castration recurrent prostate cancer. In addition, the recurrence rate is altered as a result of metastatic development and a unique histological phenotype at the primary site correlates with rise of metastases. Altogether, the CWR22 model provides an experimental system for studying the progression of and treatment for metastatic castration recurrent prostate cancer.

ACKNOWLEDGMENTS

We thank the following Roswell Park cores: Mouse Tumor Model Resource (MTMR) for assistance with animal and histology work and Pathology Resource Network (PRN) for clinical samples and data.

REFERENCES

1. SEER Stat Fact Sheets: Prostate Cancer. In: NCI, editor 2014.
2. Catalona WJ, Smith DS. 5-year tumor recurrence rates after anatomical radical retropubic prostatectomy for prostate cancer. J Urol 1994;152(5 Pt 2):1837–1842.
3. Harris WP, Mostaghel EA, Nelson PS, Montgomery B. Androgen deprivation therapy: Progress in understanding mechanisms of resistance and optimizing androgen depletion. Nat Clin Pract Urol 2009;6(2):76–85.
4. Berthold DR, Pond GR, Soban F, de Wit R, Eisenberger M, Tannock IF. Docetaxel plus prednisone or mitoxantrone plus prednisone for advanced prostate cancer: Updated survival in the TAX 327 study. J Clin Oncol 2008;26(2):242–245.
5. Tannock IF, de Wit R, Berry WR, Horti J, Pluzanska A, Chi KN, Oudard S, Theodore C, James ND, Turesson I, Rosenthal MA, Eisenberger MA, Investigators TAX. Docetaxel plus prednisone or mitoxantrone plus prednisone for advanced prostate cancer. N Engl J Med 2004;351(15):1502–1512.
6. Chen Y, Scher HI. Prostate cancer in 2011: Hitting old targets better and identifying new targets. Nat Rev Clin Oncol 2012; 9(2):70–72.
7. Chen CD, Welsbie DS, Tran C, Baek SH, Chen R, Vessella R, Rosenfeld MG, Sawyers CL. Molecular determinants of resistance to antiandrogen therapy. Nat Med 2004;10(1):33–39.
8. Gregory CW, He B, Johnson RT, Ford OH, Mohler JL, French FS, Wilson EM. A mechanism for androgen receptor-mediated prostate cancer recurrence after androgen deprivation therapy. Cancer Res 2001;61(11):4315–4319.
9. Mohler JL, Gregory CW, Ford OH, 3rd, Kim D, Weaver CM, Petrusz P, Wilson EM, French FS. The androgen axis in recurrent prostate cancer. Clin Cancer Res 2004;10(2):440–448.
10. Scher HI, Sawyers CL. Biology of progressive, castration-resistant prostate cancer: Directed therapies targeting the androgen-receptor signaling axis. J Clin Oncol 2005;23(32):8253–8261.
11. Kluetz PG, Ning YM, Maher VE, Zhang L, Tang S, Ghosh D, Aziz R, Palmby T, Pfuma E, Zirkelbach JF, Mehrotra N, Tilley A, Sridhara R, Ibrahim A, Justice R, Pazdur R. Abiraterone acetate in combination with prednisone for the treatment of patients with metastatic castration-resistant prostate cancer: U.S. Food and Drug Administration drug approval summary. Clin Cancer Res 2013;19(24):6650–6656.
12. Scher HI, Fizazi K, Saad F, Taplin ME, Sternberg CN, Miller K, de Wit R, Mulders P, Chi KN, Shore ND, Armstrong AJ, Flaig TW, Flechon A, Mainwaring P, Fleming M, Hainsworth JD,

Hirmand M, Selby B, Seely L, de Bono JS, Investigators A. Increased survival with enzalutamide in prostate cancer after chemotherapy. N Engl J Med 2012;367(13):1187–1197.

13. Wu HC, Hsieh JT, Gleave ME, Brown NM, Pathak S, Chung LW. Derivation of androgen-independent human LNCaP prostatic cancer cell sublines: Role of bone stromal cells. Int J Cancer 1994;57(3):406–412.
14. Horoszewicz JS, Leong SS, Kawinski E, Karr JP, Rosenthal H, Chu TM, Mirand EA, Murphy GP. LNCaP model of human prostatic carcinoma. Cancer Res 1983;43(4):1809–1818.
15. Horoszewicz JS, Leong SS, Chu TM, Wajsman ZL, Friedman M, Papsidero L, Kim U, Chai LS, Kakati S, Arya SK, Sandberg AA. The LNCaP cell line-a new model for studies on human prostatic carcinoma. Prog Clin Biol Res 1980;37:115–132.
16. Waters DJ, Janovitz EB, Chan TC. Spontaneous metastasis of PC-3 cells in athymic mice after implantation in orthotopic or ectopic microenvironments. Prostate 1995;26(5):227–234.
17. Kaighn ME, Narayan KS, Ohnuki Y, Lechner JF, Jones LW. Establishment and characterization of a human prostatic carcinoma cell line (PC-3). Invest Urol 1979;17(1):16–23.
18. Masumori N, Thomas TZ, Chaurand P, Case T, Paul M, Kasper S, Caprioli RM, Tsukamoto T, Shappell SB, Matusik RJ. A probasin-large T antigen transgenic mouse line develops prostate adenocarcinoma and neuroendocrine carcinoma with metastatic potential. Cancer Res 2001;61(5):2239–2249.
19. Gingrich JR, Barrios RJ, Morton RA, Boyce BF, DeMayo FJ, Finegold MJ, Angelopoulou R, Rosen JM, Greenberg NM. Metastatic prostate cancer in a transgenic mouse. Cancer Res 1996;56(18):4096–4102.
20. Ellwood-Yen K, Graeber TG, Wongvipat J, Iruela-Arispe ML, Zhang J, Matusik R, Thomas GV, Sawyers CL. Myc-driven murine prostate cancer shares molecular features with human prostate tumors. Cancer Cell 2003;4(3):223–238.
21. Wang S, Gao J, Lei Q, Rozengurt N, Pritchard C, Jiao J, Thomas GV, Li G, Roy-Burman P, Nelson PS, Liu X, Wu H. Prostate-specific deletion of the murine Pten tumor suppressor gene leads to metastatic prostate cancer. Cancer Cell 2003;4(3): 209–221.
22. Pretlow TG, Wolman SR, Micale MA, Pelley RJ, Kursh ED, Resnick MI, Bodner DR, Jacobberger JW, Delmoro CM, Giaconia JM, Pretlow TP. Xenografts of primary human prostatic carcinoma. J Natl Cancer Inst 1993;85(5):394–398.
23. Wainstein MA, He F, Robinson D, Kung HJ, Schwartz S, Giaconia JM, Edgehouse NL, Pretlow TP, Bodner DR, Kursh ED, Resnick MI, Seftel A, Pretlow TG. CW R22: Androgen–dependent xenograft model derived from a primary human prostatic carcinoma. Cancer Res 1994; 54(23):6049–6052.
24. Nagabhushan M, Miller CM, Pretlow TP, Giaconia JM, Edgehouse NL, Schwartz S, Kung HJ, de Vere White RW, Gumerlock PH, Resnick MI, Amini SB, Pretlow TG. CWR22: The first human prostate cancer xenograft with strongly androgen-dependent and relapsed strains both in vivo and in soft agar. Cancer Res 1996;56(13):3042–3046.
25. Tepper CG, Boucher DL, Ryan PE, Ma AH, Xia L, Lee LF, Pretlow TG, Kung HJ. Characterization of a novel androgen receptor mutation in a relapsed CWR22 prostate cancer xenograft and cell line. Cancer Res 2002;62(22):6606–6614.
26. Holleran JL, Miller CJ, Culp LA. Tracking micrometastasis to multiple organs with lacZ-tagged CWR22R prostate carcinoma cells. J Histochem Cytochem 2000;48(5):643–651.
27. Moser FG, Dorman BP, Ruddle FH. Mouse-human heterokaryon analysis with a 33258 Hoechst-Giemsa technique. J Cell Biol 1975;66(3):676–680.
28. Sharkey FE, Fogh J. Incidence of pathological features of spontaneous tumors in athymic nude mice. Cancer Res 1979;39-(3):833–839.
29. O'Reilly MS, Holmgren L, Shing Y, Chen C, Rosenthal RA, Moses M, Lane WS, Cao Y, Sage EH, Folkman J. Angiostatin: A novel angiogenesis inhibitor that mediates the suppression of metastases by a Lewis lung carcinoma. Cell 1994;79(2):315–328.
30. Humphrey P. Gleason grading and prognostic factors in carcinoma of the prostate. Mod Pathol 2004;17(3):292–306.

SUPPORTING INFORMATION

Additional supporting information may be found in the online version of this article at the publisher's web-site.